Latitudinal Structure of the Heliospheric Current Sheet and Corotating Streams Measured by WIND and ULYSSES

C. M. Ho[1], B. T. Tsurutani[1], J. K. Arballo[1], B. E. Goldstein[1],
R. P. Lepping[2], K. W. Ogilvie[2], A. J. Lazarus[3], and J. T. Steinberg[3]

[1] Jet Propulsion Laboratory, California Institute of Technology, Pasadena, CA 91109
[2] Laboratory for Extraterrestrial Physics, NASA/Goddard Space Flight Center, Greenbelt, MD 20771
[3] Center for Space Research, Massachusetts Institute of Technology, Cambridge, MA 02139

Submitted to Geophysical Research Letters

February 1, 1997

Abstract. All heliospheric current sheet (HCS) crossings and corotating solar wind streams detected by both WIND and Ulysses have been identified. These measurements were made when Ulysses was in its fast latitudinal scan (at a heliocentric radial distance of ~1.4 AU) and WIND was in the ecliptic plane near the Earth. Instantaneous solar wind velocities are used to map the locations of the HCS crossings and plasma sources back to the solar surface. The HCS crossing locations have been compared with those predicted by the Stanford source surface magnetic field model. In general, both locations correspond closely, but there is an error range up to 25° in heliographic longitude. These discrepancies in the HCS locations may be due to an overly southward displacement (~ 6°) in the model. WIND at ~ 6°S spent more than 55% of its time in southern hemispheric fields. We have also found that six pairs of corotating streams from 11 pairs of candidate streams have the same sources and were detected by both spacecraft at widely separated latitudes. Three pairs of streams are from the southern hemisphere, and the other three pairs come from the northern hemisphere. Under an assumption of the absence of temporal variations, a velocity gradient of $\Delta V \approx 750\, e^{-0.38\Delta\theta}$ (km/s/degree) has been determined as a function of the angular distance, $\Delta\theta$, from the HCS.

1. Introduction

The structures of the solar wind and the interplanetary magnetic field (IMF) near the ecliptic plane have been studied extensively [Hundhausen, 1977; Gosling et al., 1981; Hoeksema et al., 1983]. Using multi-spacecraft (e.g., Helios-1 and 2) measurements, the heliospheric current sheet (HCS) and IMF polarities within ±7.2° of the solar equator were identified [Villante et al., 1979; Bruno et al., 1986]. IMF measurements show a structure well ordered by heliographic longitude. However, in the low heliographic latitude region, the solar wind and IMF have very complicated three dimensional structures. High speed solar wind comes from coronal holes with near constant velocities of ~800 km/s. Low speed solar wind with an average speed of ~300 km/s at 1 AU most probably comes from the "streamer belt" region, where the magnetic field lines are closed and plasma densities are high [Gosling et al., 1981; Crooker et al., 1993]. The latitude separating two high speed flow regions has been identified as ±23.5° by recent Ulysses measurements [Gosling et al., 1995]. Within this latitude, the faster streams overtake the slower streams along an interface which approximates a spiral. Corotating interaction regions (CIRs) are formed at the interface. The HCS is embedded in the streamer belt and wraps around the Sun. Stream speeds are a function of the distance from the coronal hole boundary or from the center of the HCS [Pizzo, 1994; Gosling et al., 1995]. Stream velocity variations with latitude have been studied and modeled within a ±25° latitude range relative to the HCS [Zhao and Hundhausen, 1981; Bruno et al., 1986].

WIND was placed about the L_1 libration point of the earth in interplanetary space and monitors upstream solar wind parameters. In this study, the data we used were taken between Feb. 11 and Apr. 22, 1995 when WIND was in a region between 200 and 230 R_e upstream of earth. Corresponding to this period, Ulysses was on its way from the southern solar hemisphere toward the northern hemisphere. It took about 60 days to pass the low latitude CIR region with its perihelion at ~1.4 AU in the solar equatorial plane. This fast latitude scan provided us with unique solar wind data with large latitude coverage over a relatively short time duration [Smith et al., 1995; Gosling et al., 1995]. Figure 1 is a cartoon showing the location of both spacecraft relative to the sun during this period.

In this study, we use WIND and Ulysses measurements at different latitudes in interplanetary space to study the latitudinal structures of CIRs and the HCS. We trace plasma and magnetic field structures back to the solar surface and compare them with the

Stanford source surface model. On the basis of the identified corotating streams, the velocity gradients relative to the HCS are determined.

2. Method of Analysis

We have used the following criteria to identify all corotating interaction regions/corotating coronal streams: 1) All CIRs should have a broad density peak in the front; 2) a discernible velocity enhancement occurs next; 3) a compressed magnetic field peak lies between the density peak and velocity enhancement; 4) a clear stream leading edge is associated with a density drop, and increases of temperature and velocity; 5) in most cases. the magnetic field polarities within CIRs are the same. However, in some weak streams, not all of these features are clearly evident. Because there is no strong interaction between fast and slow streams for these cases, their interfaces could not be easily identified. We have discarded these events for this analysis and have selected only those stream events which meet the above criteria.

3. Results

Figure 2 shows the measurements of the solar wind and the IMF by WIND near earth. Three IMF components (the northward B_N, the polar angle B_θ, and the azimuthal/longitude angle B_ϕ) and the field magnitude [Lepping et al., 1995] are shown in the top four panels. The angle B_θ is defined starting from the north pole downward from 0° to 180°. Thus, the angle B_ϕ is defined starting from the opposite direction relative to the earth motion in the ecliptic plane (view from above) clockwise from 0° to 360°. When $B_\phi < 180°$, the field lines are directed toward the Sun (as in the southern hemisphere). When $B_\phi > 180°$, the field lines point away from the sun (northern hemisphere). Next are the solar wind plasma measurements [Ogilvie et al, 1995]. These data include solar wind proton speed V_{sw}, proton density N_p, and proton thermal speed, V_{th}. The 72 days of data span from Feb. 11 to Apr. 24, 1995. The corresponding solar Carrington rotations are 1892 to 1894 (Bartels rotations 2206-2208). During this period, the earth was near its minimum heliographic latitudes (6° - 7°S). Based on the variations of B_ϕ relative to 180° we have identified all of the IMF sectors (field polarities) and sector boundary crossings. The most significant feature is five high speed streams from southern coronal holes, because these streams all have magnetic fields pointing inward toward the sun. Several small streams appear between these high speed streams, because they are associated with compressed magnetic field peaks. We have determined that these small streams come from the northern hemisphere.

We have indicated each HCS crossing and CIR by an ordered index and letters. Portion of the HCS crossings have been identified by Lepping et al. [1996] in a recent study.

During this time, Ulysses was at a relative heliographic longitudinal angle of ~157° from the earth. Ulysses would be expected to observe the same solar wind streams about 12 days in advance of WIND. In Figure 3, we show the IMF and plasma measurements from Ulysses for the interval of Jan. 30 to Apr. 6, 1996 [Balogh et al., 1990; Bame et al., 1990]. The data have the same format as in Figure 1. During this period, Ulysses was between 1.42 and 1.37 AU in heliocentric radial distance, and from 25.6°S to 26.4°N in heliographic latitude. Ulysses moved out of the high speed southern coronal hole region on Feb. 4 (day 35) and entered the low latitude coronal stream region at a latitude of 23.5°S. The solar wind speed immediately dropped from ~800 km/s to ~400 km/s. Inside the latter region, Ulysses detected several CIRs and crossings of the HCS. On Mar. 27 (day 88) Ulysses left the ecliptic region and entered the northern high speed coronal region at latitude 23.5°N. Based on magnetic field observations, Ulysses encountered seven HCS crossings and ten distinct CIRs [Smith et al., 1995] inside the low latitude band (~43° wide). Plasma measurements showed nine clear coronal streams from both hemispheres [Gosling et al., 1995]. We have used letters and numbers to indicate these crossings and streams as in Figure 2.

At first glance, there seems to be no obvious relationship between the observations shown in Figure 2 and Figure 3, because they have significantly different field and plasma features. However, we can find a correlation if we trace these structures back to the solar surface. Under the assumption that solar wind streams keep the same speeds as measured by the spacecraft, we can calculate the time delay due to the solar wind radial propagation by r/V_{sw}, where r is the spacecraft's radial distance from the sun and V_{sw} is the measured instantaneous solar wind speed. We use different rotation periods (~27 days relative to earth and ~25 days relative to Ulysses) to make the heliographic longitude shifts for both spacecraft. We have mapped the IMF and plasma flows measured by WIND and Ulysses to their source points on solar surface. After these corrections have been made, the WIND data are further shifted forward (to the right) by 75° ~ 95° in heliographic longitude on the solar surface, while the Ulysses data have a shift of 80° ~ 110°.

In Figure 4, we show the relationship between measurements from the two spacecraft and solar surface maps. The solar coronal (at 1.15 solar radii) and source surface model maps are shown in the top two panels for three solar rotation cycles. Note that time runs from right to left in this plot. These charts are taken from the Solar Geophysical Data [NOAA, 1995]. The neutral line of the HCS predicted by the model is shown as a heavy curve line above the dark southern hemisphere region. The trajectories of Ulysses and WIND are also shown by heavy lines in the top panel. The next panel are WIND measurements of the IMF azimuthal angle, field magnitude, solar wind proton speed and density. The Ulysses measurements are shown at the bottom. All parameters have been corrected using locally measured solar wind speeds, and thus some distorted structures appear due to forward or backward shifts in longitude. An obvious feature is that the leading edges (with large gradients) of CIRs in the solar wind speed are extended, while the trailing edges are piled up and become steepened. We have used the vertical lines to indicate all current sheet crossings for both spacecraft, based on B_ϕ reversals. There are nine HCS crossings for WIND measurements and seven HCS crossings for Ulysses during the interval of study. The two most significant stream peaks are S_1 and S_2 originating from the south. In general, there is a consistency in the HCS crossings between the two spacecraft measurements and the current sheet crossings as portrayed on the source surface map. The HCS crossings seen in the field measurements for the two spacecraft occurred near the locations where the HCS crossings were expected in the source surface map (panel two), especially in the first two rotations. But two cycles later, there are larger differences in heliographic longitude for some crossings. For example, the No. 9 crossing for Wind has a difference of ~17°, while the error can be as large as 25° as for the No. 8' crossing for Ulysses. These discrepancies show that the source surface model may at times have errors, compared with measurements.

To study the latitudinal variations of the solar wind streams, we have identified six pairs of corotating streams which come from the same sources and were detected by both spacecraft at different latitudes, from 11 pairs of candidate streams. Three pairs of streams are from the southern hemisphere, while the other three pairs are from the northern hemisphere. The remaining five pairs of streams (S_0, N_0, S_3, N_3, and N_5) do not have complete CIR features and are excluded from this data base. In Figure 5a and b, we have shown the variations of the stream velocities and their velocity gradients for the six streams. We assume that there is no temporal variation for these streams. Thus, their speed variations will be due only to the latitudinal differences of the two spacecraft. We have used their speed in the trailing edge as their original speeds to avoid the speed changes due to the stream interaction. We also do not distinguish if the streams are from extended polar coronal holes or from isolated low latitude holes. In Figure 5a, we have shown the speed and latitude values for each stream detected by both spacecraft. The slopes of the lines connecting both velocity values give the velocity gradients with latitude. We find good alignment for the six pairs of streams. For a stream from the southern hemisphere, its speed is always detected with higher values at more southerly latitudes, while for a stream from the northern hemisphere, higher speeds are seen at more northerly latitudes. An overlapping in the heliographic latitude for both hemisphere streams is due to movement up and down of the neutral line. Because it is relatively difficult to determine the boundary location of the coronal holes, we have shown the speed gradients as a function of the angular distance from the HCS in Figure 5b. Velocity gradients (ΔV) decrease rapidly with increasing average angular distance ($\Delta\theta$) from the HCS. The angular distance between the spacecraft and the HCS varies, following the peaks and troughs of the HCS. For stream S_4, there is the largest latitude separation (~20°) of the two spacecraft. The velocity variation may be fitted using an exponential curve, $\Delta V = 750\ e^{-0.38\Delta\theta} + 6$ (km/s/degree). There is a high (47 km/s/degree) velocity gradient in the location close to the HCS for stream S_2. In the regions with an angular distance greater than 20° from the HCS, the velocity gradients become small.

4. Discussion

During the three solar rotations, the HCS showed a wavy, four-sector structure. The Stanford source surface model indicated that the center of the HCS on average has a southward shift of about 6° (see panel 2 of Figure 4). The neutral line has a maxima at 24°N and a minima at 36°S. During this period, earth was located at 6°-7°S latitude, almost in the central location of the HCS. If the southward displacement shown by this model is correct, WIND should be almost equally in the north and south sectors. Our statistical results show that the ratio between the north sector and south sector durations is 1:1.15. WIND spent slightly more time in the south sector. This shows that the model has an excessive southward displacement. This displacement may cause some inconsistencies between the measurements from two spacecraft and the model in HCS crossing locations. If this displacement is reduced, we will find that sector boundary 6' for Ulysses will be much closer to the HCS crossings. This may explain why Ulysses did not detect a north polarity field when it was at above the HCS minima of the model in cycle 1892. Ulysses probably was in a position below the HCS minima during the interval. It may also partially explain why WIND detected the high speed streams mostly from the southern hemisphere, because it mainly stayed southward of the central HCS. However, the streams from the northern coronal holes are indeed there but weak. The northern coronal holes are probably located in higher latitude regions, while southern coronal holes have extended up to equatorial regions.

Previous studies [Zhao and Hundhausen, 1981; Bruno et al., 1986] were based on data detected within ±7.2° in heliographic latitude relative to the equator (in the ecliptic plane), or ~±30° latitude range relative to the HCS. In this study, Ulysses had reached ±23° regions in heliographic latitude (the angular distance from the HCS has extended to ~±40°). Thus we have extended solar wind stream measurements to a much larger latitude range. In the studies of Zhao and Hundhausen [1981] and Bruno et al. [1986], it was found that solar wind speed has a trough about ±20 ~ ±30° wide relative to the center of the HCS. The bottom speed of the trough is about 400 km/s, while the top is ~ 650 km/s. The gradient in speed varies from 5 to ~15 km/s/deg. In our model, the gradient in stream speed has an exponential form as $750\ e^{-0.38\Delta\theta}$ as a function of angular distance from the HCS. After an integration, we can also obtain an exponential type of speed profile with a cut-off speed (e.g., 750 km/s). The turning point (velocity trough width) of the speed profile is at about ±20°. This result is similar to that from the statistical study based on Helios-1 and 2 [Bruno et al., 1986]. However, in the region close to the HCS, our measurements show a much larger gradient (46 km/s/deg), while in the region far from the HCS, the gradient still exists. The differences may be due to that we have used an average (or central) angular distance, instead of a real distance from the HCS for the gradient. Actually, the speed variations can take place anywhere between two spacecraft.

We also note that during this period almost every large CIR (mainly high speed streams from the south) generates a recurrent storm (not shown in this paper). During the solar declining phase, it is suggested that high speed streams and IMF B_z fluctuations associated with Alfven waves are the main causes of these minor and moderate recurrent storms [Tsurutani et al., 1995] (this will a topic for our future study).

5. Summary

The measurements from WIND and Ulysses at different latitudes provide an opportunity to study latitudinal variations of the IMF and solar wind streams. We have compared these measurements made in interplanetary space with the source surface model and coronal synoptic charts. After mapping these solar wind structures to the solar surface, we find that the HCS crossings detected by both spacecraft appear to be near the expected locations in the solar surface map. However there are differences (up to 25°) in heliographic longitude for some crossings. These differences may be due to an over-displacement southward for the source surface model or mapping errors (stream speed variations, and non-radial flows) in this study. Because WIND had a slightly longer duration in the sector with magnetic polarity of the southern hemisphere pole when it stayed at ~6°-7°S, the average center of the HCS should be closer to the heliographic equatorial plane, instead of a southward displacement as the source surface model predicted.

Even though the spacecraft (WIND and Ulysses) were on nearly opposite sides of the sun, they detected what appeared to be the same high speed stream at different radial distances. Based on the corotating stream criteria, from 11 pairs of potential streams, we have identified six pairs of corotating streams which come from the same sources. Using these streams, the velocity gradients as a function of angular distance from the HCS are determined. Under an assumption of no temporal variations, the velocity gradients may be expressed as an exponential form as $\Delta V \approx 750\ e^{-0.38\Delta\theta}$ (km/s/degree). Similar to previous studies, this profile shows that the solar wind speed trough has a width of about ±20° around the HCS. However, we see a very large gradient (46 km/s/deg) in the region close to the HCS, and a small gradient at a large distance (20°-40°) from the HCS.

Acknowledgments: We thank Dr. X.-P. Zhao for providing the Stanford source surface model data. C.M.Ho also thanks Dr. E.J.Smith for constructive discussions. The research conducted at the Jet Propulsion Laboratory, California Institute of Technology was performed under contract to the National Aeronautics and Space Administration.

References

Balogh, A., et al., The magnetic field investigation on the Ulysses mission: Instrumentation and preliminary scientific results, *Astron. Astrophys. Supp. Ser. 92*, 221, 1992.

Bame, S.J. et al., The Ulysses solar wind plasma experiment, *Astron. Astrophys. Supp. Ser. 92*, 237, 1992.

Bruno, R. et al., In-situ observations of the latitudinal gradients of the solar wind parameters during 1976 and 1977, *Solar Physics, 104*, 431, 1986.

Crooker, N. U., G. L. Siscoe, S. Shodhan, D. F. Webb, J. T. Gosling, and E. J. Smith, Multiple heliospheric current sheets and coronal streamer belt dynamics, *J. Geophys. Res., 98*, 9371, 1993.

Gosling, J. T., et al., Coronal streamers in the solar wind at 1 AU, *J. Geophys. Res., 86*, 10049, 1981.

Gosling, J. T. et al., The band of solar wind variability at low heliographic latitudes near solar activity minimum: Plasma results from the Ulysses rapid latitude scan, *Geophys. Res. Lett., 22*, 3329, 1995.

Hoeksema, J. T. et al., The structure of the heliospheric current sheet: 1978-1982, *J. Geophys. Res., 88,* 9910, 1983.

Hundhausen, A.T., An interplanetary view of coronal holes, in *Coronal holes and high speed Wind Streams*, edited by J. B. Zirker, Press, Boulder CO, 225, 1977.

Lepping, R. P. et al., The WIND magnetic field investigation, *Space Sci. Rev., 71*, 207, 1995.

Lepping, R. P. et al., Large-scale properties and solar connection of the heliospheric current and plasma sheets: WIND observations, *Geophys. Res. Letts., 23*, 1199, 1996.

NOAA, Solar-Geophysical Data, Edt., H.E.Coffey, No. 610 -Part 1, June 1995.

Ogilvie, K. W. et al., SWE, A comprehensive plasma instrument for the WIND spacecraft, *Space Sci. Rev., 71*, 55, 1995.

Pizzo, V. J., Global, quasi-steady dynamics of the distant solar wind. 1. Origin of north-south flows in the outer heliosphere, *J. Geophys. Res., 99,* 4173, 1994.

Smith, E. J. et al., Results of the Ulysses fast latitude scan: Magnetic field observations, *Geophys. Res. Lett., 22,* 3325, 1995.

Villante, E. et al., The shape and location of the sector boundary surface in the inner solar system, *J. Geophys. Res., 84,* 6641, 1979.

Tsurutani, B. T. et al., Interplanetary origin of geomagnetic activity in the declining phase of the solar cycle, *J. Geophys. Res.*, *100,* 21717, 1995.

Zhao, X. P., and A. J. Hundhausen, Organization of solar wind plasma properties in a tilted, heliomagnetic coordinate system, *J. Geophys. Res.*, *86*, 5423, 1981.

Figure captions

Figure 1. A cartoon showing the locations of WIND and Ulysses during the period of this study. WIND was near the equinox and at southern solar latitudes (~ 6°S), while Ulysses was traversing from the southern to the northern hemisphere with a 1.4 AU perihelion at the solar equator. WIND detected the same solar stream about 12 days after Ulysses.

Figure 2. Magnetic field and solar wind plasma measured by WIND near the L1 point of earth. Crossings of the HCS are indicated by vertical lines at B_ϕ reversals and are numbered sequentially 1 through 9. All streams observed from both hemispheres are numbered using letters S (from the south) and N (from the north).

Figure 3. Ulysses measurements of IMF and solar wind plasma in interplanetary space at around 1.4 AU. During this time, Ulysses was experiencing a fast latitude scan from the southern to northern hemisphere. Near the ecliptic plane, it detected 10 interaction streams. The crossings and streams are numbered in an order corresponding to the WIND measurements.

Figure 4. A comparison between a solar coronal chart, source surface map and observations by both spacecraft at different latitudes. Measurements from both spacecraft have been mapped back to the footprints on the solar surface. We see a general consistency for the HCS crossing locations between the spacecraft measurements and the model predictions within certain errors. All streams with the same sources and field polarities have been identified.

Figure 5. Latitudinal velocity variations for the six pairs of corotating streams. a) Velocity variations are aligned in each side of the HCS. The slopes give velocity gradients. b) Velocity gradients quickly decrease as the average angular distance from the HCS increases. This variation is fitted by an exponential function. The horizontal bars give the error ranges in latitudes.

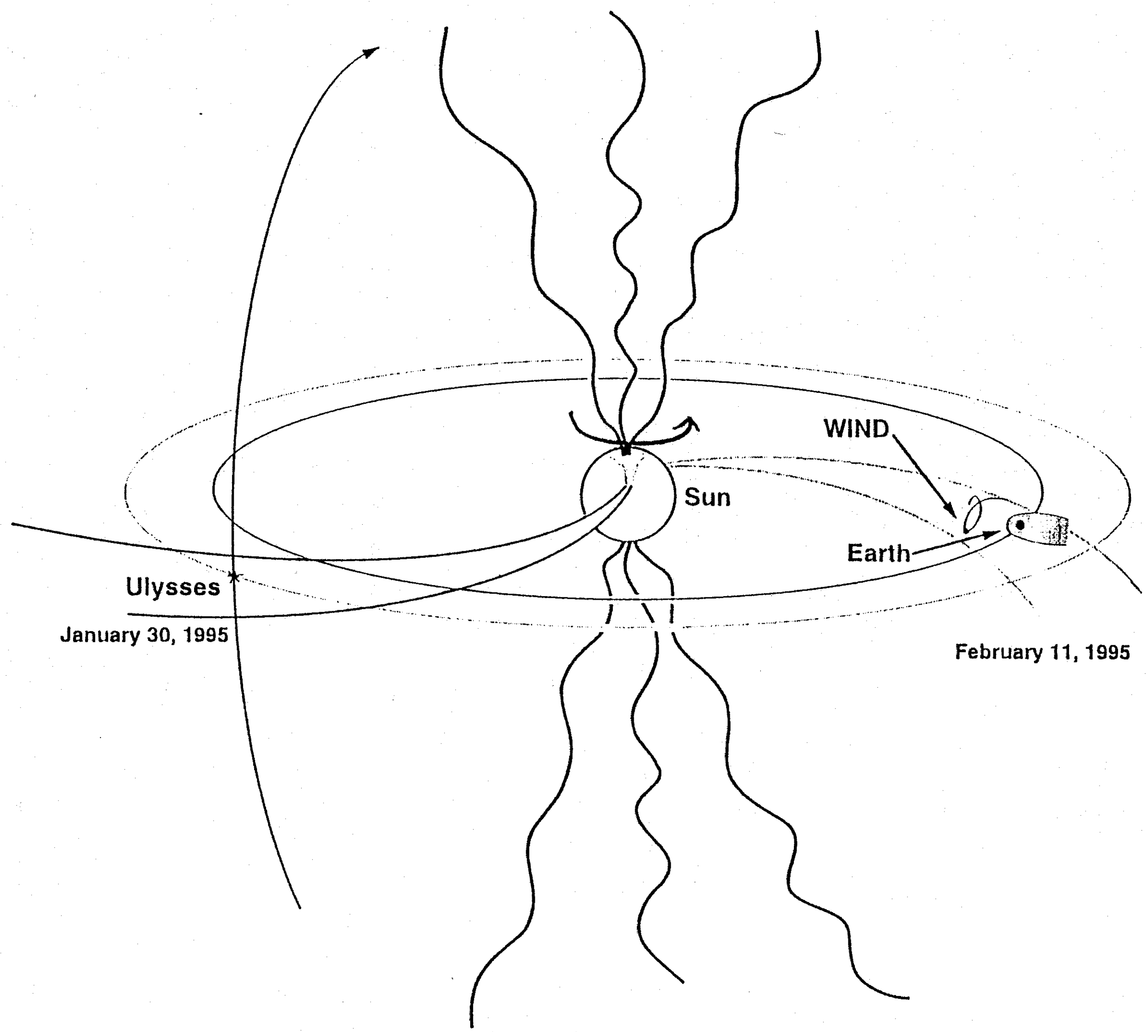

Figure 1

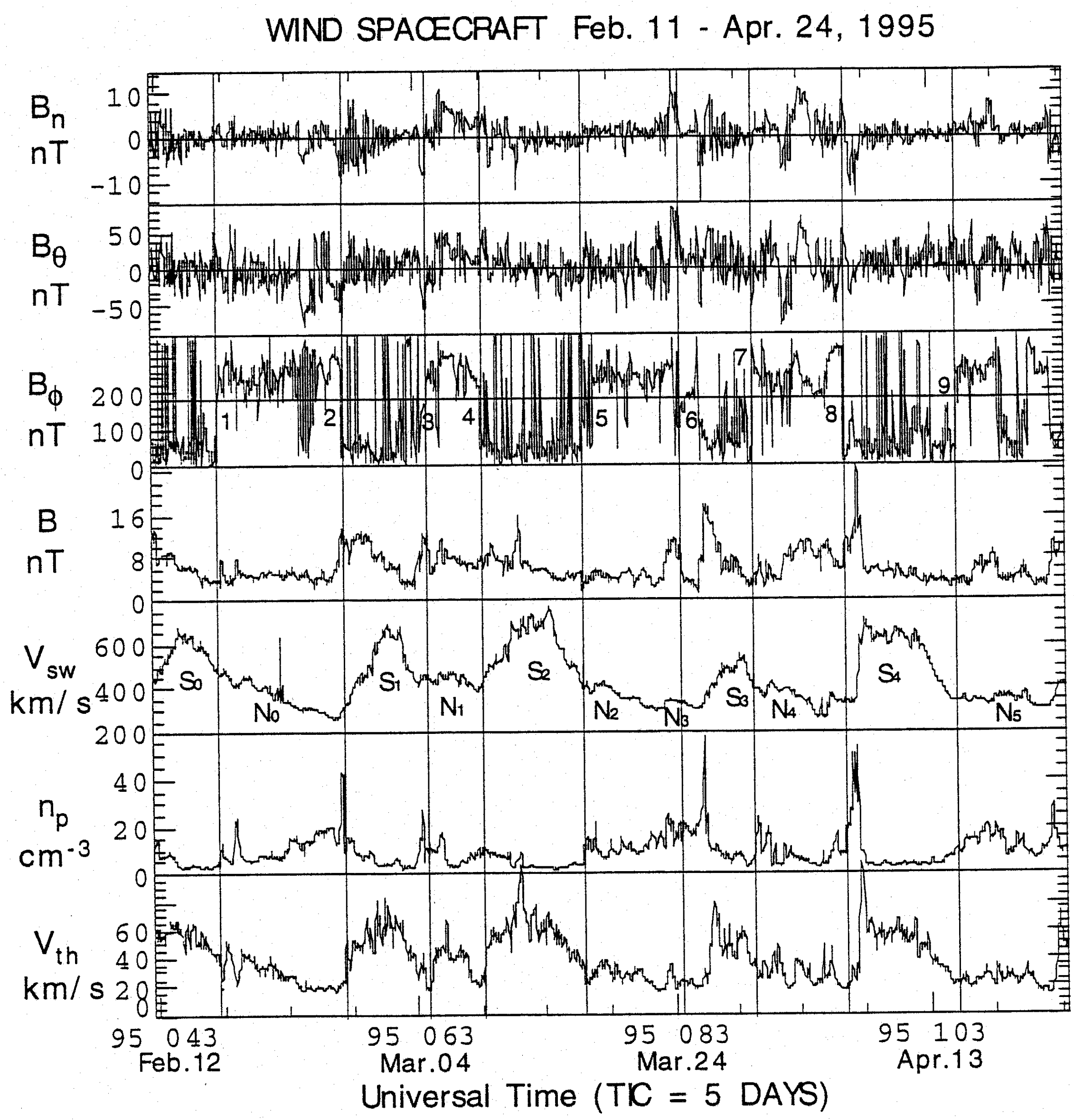

WIND SPACECRAFT Feb. 11 - Apr. 24, 1995
Bn nT
10
0
-10
Bθ nT
50
0
-50
Bφ nT
200
100
0
1
2
3
4
5
6
7
8
9
B nT
16
8
0
Vsw km/s
600
400
200
S0
S1
S2
S3
S4
N0
N1
N2
N3
N4
N5
np cm-3
40
20
0
Vth km/s
60
40
20
0
95 043
Feb.12
95 063
Mar.04
95 083
Mar.24
95 103
Apr.13
Universal Time (TIC = 5 DAYS)

Figure 2

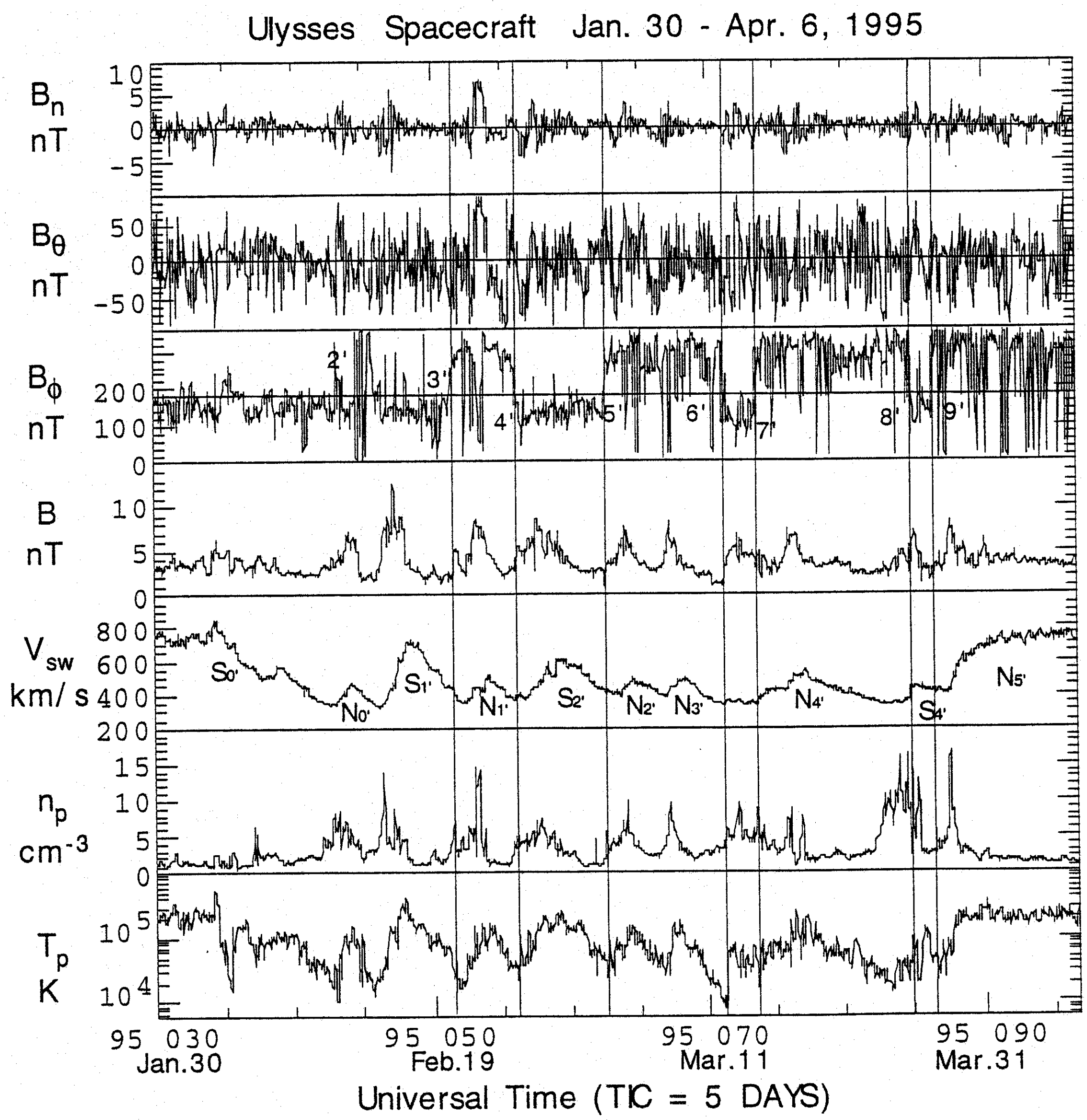

Ulysses Spacecraft Jan. 30 - Apr. 6, 1995
Bn nT
Bθ nT
Bφ nT
B nT
Vsw km/s
np cm-3
Tp K
S0' N0' S1' N1' S2' N2' N3' N4' S4' N5'
2' 3' 4' 5' 6' 7' 8' 9'
95 030 Jan.30
95 050 Feb.19
95 070 Mar.11
95 090 Mar.31
Universal Time (TIC = 5 DAYS)

Figure 3

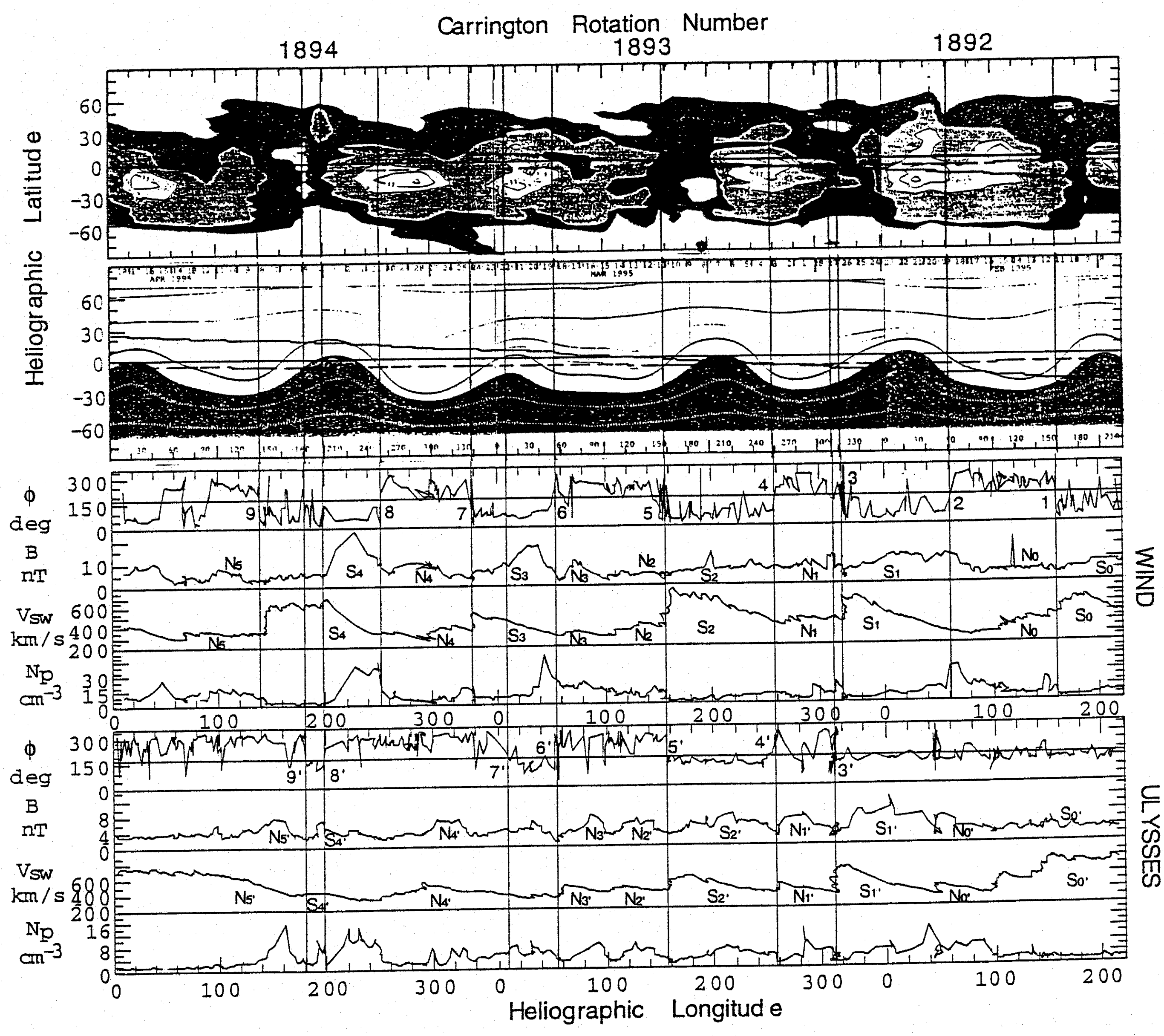
Carrington Rotation Number
1894
1893
1892
Heliographic Latitude
φ deg
B nT
Vsw km/s
Np cm-3
WIND
ULYSSES
Heliographic Longitude

Figure 4

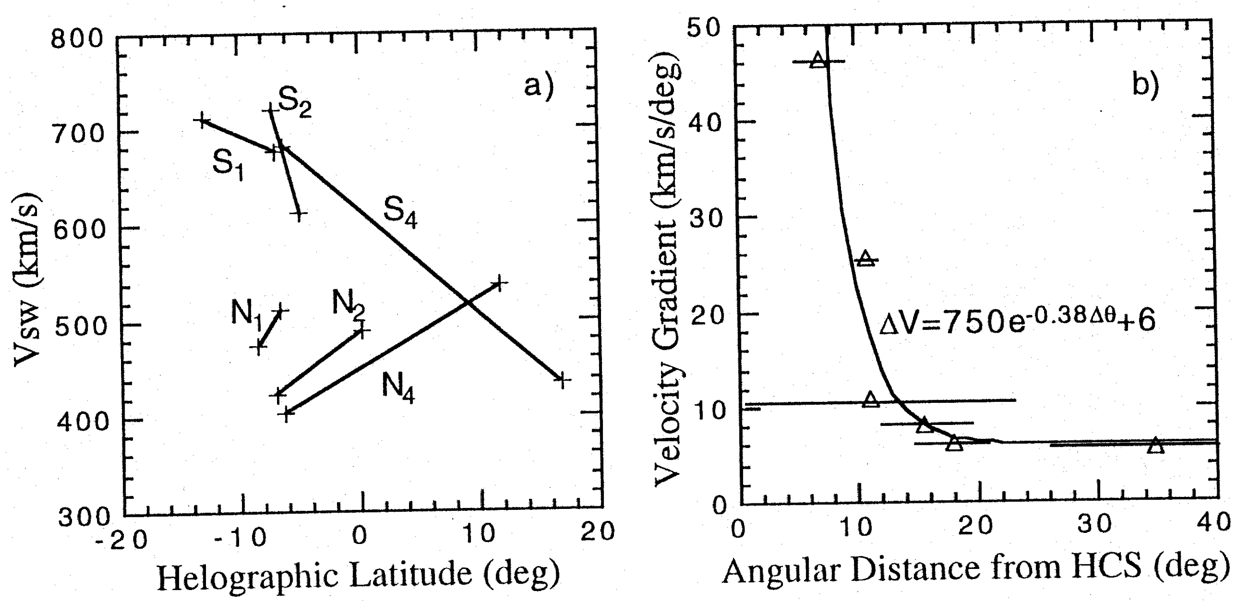
a)
Vsw (km/s)
800
700
600
500
400
300
-20
-10
0
10
20
Helographic Latitude (deg)
S1
S2
S4
N1
N2
N4
b)
Velocity Gradient (km/s/deg)
50
40
30
20
10
0
0
10
20
30
40
Angular Distance from HCS (deg)
ΔV=750e-0.38Δθ+6

Figure 5